

Received April 23, 2020, accepted May 5, 2020, date of publication May 8, 2020, date of current version May 20, 2020.

Digital Object Identifier 10.1109/ACCESS.2020.2993263

Multi-Objective Optimization for Coordinated Day-Ahead Scheduling Problem of Integrated Electricity-Natural Gas System With Microgrid

J. H. ZHENG^{ID}, (Member, IEEE), C. Q. WU, J. HUANG, Y. LIU^{ID}, (Member, IEEE),
AND Q. H. WU^{ID}, (Fellow, IEEE)

School of Electric Power Engineering, South China University of Technology, Guangzhou 510640, China

Corresponding author: Y. Liu (epyangliu@scut.edu.cn)

This work was supported in part by the National Key R&D Program of China under Grant 2018YFE0208400, in part by the Natural Science Foundation of Guangdong Province, China, under Grant 2018A030313799, and in part by the Fundamental Research Funds for the Central Universities.

ABSTRACT This paper presents a multi-objective optimization algorithm for coordinated day-ahead scheduling problem of integrated electricity-natural gas system with microgrid (IENG-S-M). Mathematically, the day-ahead scheduling of IENG-S-M is formulated as a multi-objective optimization problem considering multitudinous constraints. In order to solve the problem efficiently, we introduce an acceleration of differential evolution, Lévy search strategy and a treatment mechanism to multitudinous and complex constraints into the original Non-dominated Sorting Genetic Algorithm-III (NSGA-III). Furthermore, a decision making method based on a fuzzy function approach is used to determine a final optimal solution from the Pareto-optimal solutions. Simulation studies are carried out on a modified IEEE 39-bus system and 15-node gas system to verify the effectiveness of the modified NSGA-III (MNSGA-III), in comparisons with the NSGA-II and NSGA-III. The simulation results show that the Pareto-optimal solutions obtained by MNSGA-III has better convergence performance and diversity than the NSGA-II and NSGA-III.

INDEX TERMS Multi-objective optimization, differential evolution, Lévy search strategy, MNSGA-III, integrated energy systems.

I. INTRODUCTION

WITH the growing concerns over the climate change and energy security around the world, more and more attention is being paid to the development and utilization of the integrated energy system (IES). As the increasing penetration of renewable energy sources, the interconnections of distributed renewable energy will bring a huge impact on the operation of electricity network and gas network, and the coordination of IES will face severe challenges [1], [2].

Over the last decades, a number of methods have been developed to solve the optimization problems. In general, these methods can be divide into mathematics-based optimization methods and heuristic methods [3], [4]. Mathematics-based optimization methods including linear programming [5], non-linear programming [6], [7], mixed

integer linear programming [8], mixed integer non-linear programming [9], [10]. Some of the mathematics-based optimization methods can solve this problem very fast. However, these methods have some disadvantages when dealing with non-linear, non-smooth and non-convex day-ahead scheduling problem. Moreover, these methods are sensitive to the choice of the initial values and may be fail into local optimum due to the improper initial points. Heuristic methods have aroused intense interest due to their versatility, flexibility, and robustness in seeking the global optimum solution, such as GSO [11], PSO [12], DE [13], GSA [14], and etc. Attempts have been made to apply these algorithms, including machine-learning algorithms, to tackle large-scale and economically important optimisation problems, such as optimal power flow and economic dispatch in power systems [15].

In recent years, NSGA-III, which proposed by Deb *et al.* [16], [17], has been show perfect performance for

The associate editor coordinating the review of this manuscript and approving it for publication was Huai-Zhi Wang^{ID}.

a number of different types of benchmark functions and multi-objective problems. What's more, Mkaouer *et al.* proposed for the first time a scalable search-based software engineering approach based on this newly proposed evolutionary optimization method NSGA-III, which addresses software engineering problems when a large number of objectives are to be optimized [18], [19]. The authors of reference [20] presented an extended NSGA-III algorithm to select new generation by introducing the dominance relationship criterion based on constraint violation. The superior quality and good distribution of the Pareto-optimal solutions show the NSGA-III can find an efficient alternative for optimizing multi-objective economic emission hydro-thermal-wind scheduling problem. Reference [21] proposed an orthogonal design-based non-dominated sorting genetic algorithm-III (ONSGA-III) to optimize the lockage co-scheduling of Three Gorges Dam and Gezhou Dam. An improved non-dominated sorting genetic algorithm is proposed by Chen to solve reservoir flood control operation problem [22]. Reference [23] proposed improved NSGA-III based on objective space decomposition for enhance the convergence of NSGA-III and tested it on number of many-objective optimization problems with state-of-the-art algorithms. In 2016, Bhesdadiya *et al.* employed the NSGA-III algorithm to solve multi-objective combined economic emission dispatch problem [24]. The experimental and practical results all show perfect performance of the NSGA-III. However, there is still an insufficiency in NSGA-III algorithm, which emphasized the diversity but neglected the speed of convergence and the ability of exploitation.

Inspired by the NSGA-III algorithm, this paper proposes a MNSGA-III algorithm by introducing an acceleration of differential evolution, Lévy search strategy to mitigate the imperfections of original NSGA-III algorithm. The acceleration of differential evolution is applied to accelerate the searching process and enhance the diversity at the same time. Compared with random walk, Lévy search strategy is more efficient, due to it can escape away from the local optimum to find well-distributed Pareto-optimal solutions in search process. In the proposed MNSGA-III algorithm, we use the Lévy search strategy to improve the ability of exploitation. Moreover, a treatment mechanism is applied to solve multi-objective optimization problem which contains multitudinous and complex constraints. To verify the efficiency of the proposed algorithm, the MNSGA-III is tested on the day-ahead scheduling problem of IENGs-M system, and the results obtained by the MNSGA-III are compared with those by other reported methods.

The rest of this paper is organized as follows: Section II presents the multi-objective operation optimization for the IENGs-M. Section III introduces the framework of the MNSGA-III in details. A fuzzy function approach is presented in Section IV. Simulation results and comparisons are given in Section V. Finally, the last section draws the conclusion of this paper.

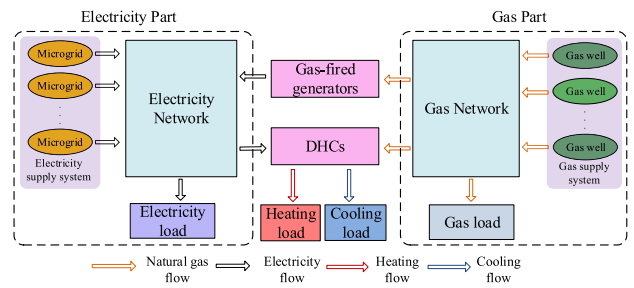


FIGURE 1. The structure of the IENGs-M system.

II. PROBLEM FORMULATION

A. FRAMEWORK OF IENGs-M

The framework of IENGs-M system considered in this paper is shown in Fig. 1. As shown in the figure, the IENGs-M consists of electricity network, natural gas network, distributed heating and cooling stations (DHCs). Specifically, the electricity network and natural gas network are connected by the gas-fired generators. Furthermore, microgrids are connected to the electricity network to embed distributed renewable energy resources. Consequently, the aim of the multi-objective operation problem of IENGs-M is to determine an optimal energy scheduling over a day-ahead period of time that minimizes the operation cost and emissions subject to several constraints simultaneously.

The electricity part includes electricity network, electricity load, and the electricity supply system-microgrids. Each microgrid consists of wind turbine (WT) generators, photovoltaic generators (PV), diesel generators (DG), which is shown in Fig. 2. The gas part includes gas supply system, gas network, and gas load.

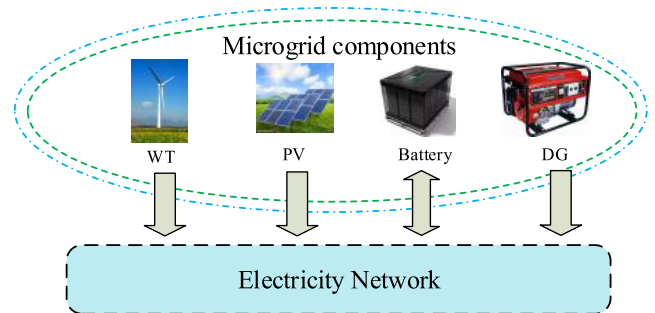


FIGURE 2. The components of the microgrid in the IENGs-M system.

B. OBJECTIVE FUNCTIONS

In this paper, two objective functions in the multi-objective operation of the IENGs-M are defined and minimized at the same time which can be formulated as follows:

$$\begin{aligned} \min & [J_1(X, Y), J_2(X, Y)] \\ \text{s.t.} & h(X, Y) = 0 \\ & g(X, Y) \leq 0 \end{aligned} \quad (1)$$

J_1 and J_2 represent the total operation cost and the pollution of the IENGs-M system, respectively. $h(X, Y)$ and $g(X, Y)$ denote the constraints.

1) TOTAL OPERATION COST

The total operation cost of the IENGs-M includes the operation cost of electricity network and the operation cost of gas network. At the same time, the voltage offset is taken into consideration to make electricity network operate in a safe state. The objective function is shown in (2) which represents the total operation cost of the IENGs-M, while (3), (4) and (5) represent the cost of electricity network, the cost of gas network and the penalty term of voltage set, respectively. The cost of electricity network considers the start-up and show-down cost of the wind/PV/battery/generation units. The $\varphi(x)$ in the penalty term of voltage set is described by (6).

$$\min J_1 = \sum_{t=1}^T [C_{En}(t) + C_{Gn}(t)] + \Delta V \quad (2)$$

$$C_{En}(t) = \sum_{j=1}^{N_1} [u_{j,t} \cdot x_{en,j}(t) B_j + S_{j,start} \times \max(0, u_{j,t} - u_{j,t-1}) \cdot x_{en,j}(t) + S_{j,shut} \times \max(0, u_{j,t-1} - u_{j,t}) \cdot x_{en,j}(t)] \quad (3)$$

$$+ \sum_{j=1}^{N_2} (a_j^{DG} P_{j,t}^2 + b_j^{DG} P_{j,t} + c_j^{DG}) \quad (4)$$

$$C_{Gn}(t) = \sum_{j=1}^{N_3} Q_{W,t}^j \cdot Cost_{gas,j,t} \quad (4)$$

$$\Delta V = \sum_{t=1}^T \sum_{i=1}^n (\varphi(|V_{i,t} - V_i^{ref}| - \delta V_i)) / V_i \quad (5)$$

$$\varphi(x) = \begin{cases} 0 & \text{if } x < 0 \\ x & \text{else} \end{cases} \quad (6)$$

T is the total scheduling period. N_1 is the total number of wind/PV/battery/generation units. N_2 is the number of DG. N_3 is the number of gas sources. $u_{j,t}$ is the status of wind/PV/battery/generation unit j at time t . $x_{en,j}$ is the power output of j th wind/PV/battery/generation units at time t . B_j is the operation cost of j th generation units. $S_{j,start}$ and $S_{j,shut}$ are the start-up and shut-down cost for j th generation units. $Q_{W,t}^j$ is the amount of j th gas sources at time t . $Cost_{gas,j,t}$ is the gas purchase cost of supplier i at time t . n is number of electricity network nodes. $V_{i,t}$ is the voltage magnitude of node i at time t . V_i^{ref} is the anticipant voltage magnitude of node i which is taken as 1.0 p.u. in this paper, δV_i is the permitted maximum voltage deviation of node i which is set 0.05 p.u.

2) POLLUTION

The second objective function is the pollution of the IENGs-M. Four of the most pollutants are considered in this objective function: CO, CO₂, SO₂, NO_x. The mathematical

formulation of the pollutant function is described in (7)-(9).

$$\min J_2 = \sum_{t=1}^T [E_{En}(t) + E_{Gn}(t)] \quad (7)$$

$$E_{En}(t) = \sum_{i=1}^{N_1+N_2} \sum_{g=1}^G \psi^g \cdot E_{elec}^{i,g} \cdot P_{i,t} \quad (8)$$

$$E_{Gn}(t) = \sum_{i=1}^{N_3} \sum_{g=1}^G \psi^g \cdot E_{gas}^{i,g} \cdot Q_{W,i}^t \quad (9)$$

where $P_{i,t}$ denotes the output power of i th generation units at time t . G is the number of the types of pollutant emissions. ψ^g represents the amercement of the g th type of atmospheric pollutant emission. $E_{elec}^{i,g}$ and $E_{gas}^{i,g}$ represent the emission rate of g th type pollutant emitted by i unit in electricity and natural gas network, respectively.

III. MODIFIED NSGA-III ALGORITHM

A. NSGA-III ALGORITHM

The NSGA-III, which proposed by Deb et al. [16], [17] utilizes the fast non-dominated sorting concept, elitism, a set of well-distributed reference points to update the obtained solutions of diversity preservation. The detail description of the NSGA-III steps are given in [16] and the main procedure of NSGA-III is briefly described below.

1) POPULATION INITIALIZATION

At the first step, SN numbers of D -dimensional individuals are generated randomly. Every single individual in the initial population of the solutions is also randomly generated using uniform random numbers ranging over the feasible limits of each control variable by using the following expression:

$$x_{i,j} = x_j^{\min} + \text{rand}(0, 1) * (x_j^{\max} - x_j^{\min}) \quad i = 1, 2, \dots, SN \quad j = 1, 2, \dots, D \quad (10)$$

where D is number of optimization parameters. x_j^{\min} and x_j^{\max} are the lower and upper limits of the j th dimension, respectively. $\text{rand}(0, 1)$ is a uniformly distributed random number between 0 and 1.

2) GENERATE REFERENCE POINTS ON A HYPER-PLANE

The predefined set of reference points are used to ensure diversity of the obtained solutions. In this paper, Das and Dennis's systematic approach that produces points on a normalized hyper-plane is used. If p divisions are considered along each objective, the total number of reference points (H) in an M -objective problem is given by

$$H = \binom{M+p-1}{p} \quad (11)$$

usually, the number of H is directly related to the desired number of trade-off points.

3) TOURNAMENT SELECTION OF PARENT POPULATION

At the i th generation, the parent population is P_t and its size is SN . Then the parent population P_t is divided into different non-domination levels (F_1, F_2, \dots, F_l) based on non-dominated sorting. In addition to front rank, a new parameter called crowding distance is also calculated for each individual which is a measure of how close the individual is to its neighbors in the objective function. The larger value of the crowding distance is, the better diversity of individual is. Then pre-offsprings are selected from the parent population by applying Binary Tournament Selection based on non-dominated operator ($<_n$). Non-dominated operator is based on front level and crowding distance as follows:

- 1) The individual with lower front rank value is greater than the other regardless of crowding distance, and it's selected.
- 2) The individual is selected with the larger crowding distance when two individuals located in the same front.

4) CROSSOVER AND MUTATION

The offspring population (Q_t) is created after the operation of Simulated Binary Crossover and mutation to the pre-offspring. Thereafter the combined populations of parents and offspring ($S_t = P_t \cup Q_t$) are sorted again based on non-domination.

5) NORMALIZATION OF OBJECTIVE FUNCTION

Before associating the combined populations with the reference points, the objective functions of the combined populations need to be normalized so they have an identical range. Firstly, calculate the ideal point obj^{min} by finding the minimum corresponding objective value. Secondly, convert to the new objective value by subtracting the objective value obj with the ideal point obj^{min} . Thirdly, calculate the extreme points by identifying the solutions that make the achievement scalarization function minimum. Note that the achievement scalarization function here is formed with the objective value obj and the weight vector close to the corresponding objective value. Then, calculate the intercept points a_{obj} . These points are the interception between the corresponding objective values with its corresponding extreme points obtained from the last step. Lastly, normalize the objective values with the following equation:

$$norm(obj.i) = \frac{obj.i - obj.i^{min}}{a_{obj.i}}, \quad i = 1, 2, \dots, M \quad (12)$$

when a hyper-plane is constructed, it will yield $\sum_{i=1}^M norm(obj.i) = 1$, where M is the number of objective functions.

6) SELECTION BASED ON REFERENCE POINTS

After normalizing all the objective values in S_t , it need to associate them with the reference points. Firstly, the perpendicular distance between individual in S_t and each of reference lines, which is constructed by joining the ideal point

with the reference point, is calculated. Each individual in S_t is then associated with a reference point having the minimum perpendicular distance. Finally, the niche-preservation operation which plays an important role in maintaining the diversity of the solutions is used to select members from F_l . For the j th reference point, the niche count ρ_j is the number of the individuals form S_t/F_l that are associated with the j th reference point. The reference point having the minimum niche count is identified and the member from the last front F_l which is associated with the minimum niche count is included in the final population. The niche count of the identified reference point is increased by one and the procedure is repeated to fill up population S_{t+1} .

B. MODIFIED NSGA-III ALGORITHM

1) ACCELERATION OF DIFFERENTIAL EVOLUTION

The search space exploration of NSGA-III is executed by the operation of crossover and mutation. The parent population seeks the optimal solution along their way until the offspring population, which is created by Simulated Binary Crossover, dominated the parent population. But this is not conducive to raise the convergence speed and optimization efficiency to some extent. In this paper, a selection of DE algorithm is applied as the acceleration operation to accelerate the searching process and enhance the diversity of the populations in the approach. In order to enhance the search efficiency, DE/best/1/bin is adopted. The individual which is the best of the three randomly selected different parent individuals is regarded as their donors. Hence, the individuals at the m th iteration in the operation are produced as follows:

$$x_{i,j}^{m+1} = \begin{cases} \text{if rand}(1) < R_{acc} \\ x_{best,j}^m + F_{acc} * (x_{r1,j}^m - x_{r2,j}^m) \\ \text{otherwise} \\ x_{i,j}^m \end{cases} \quad \begin{matrix} i = 1, 2, 3, \dots, Np \\ j = 1, 2, 3, \dots, D \\ m = 0, 1, 2, \dots, iteration_{max} \end{matrix} \quad (13)$$

where F_{acc} is the scaling factor, R_{acc} is the crossover factor, Np is number of the operation that is equal to the number of the parent populations, D is the number of optimization parameters, $iteration_{max}$ represents the maximum iteration, $r1$, $r2$ and $best$ identify three different random numbers uniformly distributed in $[1, Np]$, the best is selected from the three individuals based on non-dominated operator. The offspring will replace its parents as the rank of the offspring is better than the parents, or based on the reference points the offspring's diversity is better than the parents. To our knowledge, the operation of DE acceleration has not been employed in the way described in our approach for the Multi-objective problem.

2) LÉVY FLIGHT STRATEGY

Lévy flight is random walk that is named after Paul Lévy, a French mathematician. Various studies have shown that

flight behavior is more efficient than the random walk, because Lévy flight owns an inverse square power-law distribution of flight lengths. The symmetrical Lévy stable distribution can be defined as:

$$L_{\lambda,\gamma} = \frac{1}{\pi} \int_0^\infty e^{-\gamma q^\lambda} \cos(qy) dq \quad (14)$$

where $y \in R$, $0 \leq \lambda \leq 2$ defines the index and determines the shape of the distribution. $\gamma > 0$ is a scaling factor that selects the scale unit of the distribution. By Lévy flight strategy, offspring of the population is calculated as:

$$x^{m+1} = x^m + \alpha \oplus Levy(\beta) \quad (15)$$

where α is the step size which is related to the scales of the problem of interest. In the proposed approach, α is random number for all dimensions of the individuals. Combining the Lévy flight strategy with the acceleration of DE, equation (13) will be transformed into:

$$x_{i,j}^{m+1} = \begin{cases} \text{if } \text{rand}(1) < R_{acc} \\ x_{best,j}^m + \text{stepsize}_j * (x_{r1,j}^m - x_{r2,j}^m) \\ \text{otherwise} \\ x_{i,j}^m \end{cases}$$

$$i = 1, 2, 3, \dots, Np \quad j = 1, 2, 3, \dots, D$$

$$m = 0, 1, 2, \dots, \text{iteration}_{max} \quad (16)$$

when the current number of iteration is considered in the step-size, the equation which is adjusted along with the iteration will be converted to as follows:

$$\text{stepsize}_j = \text{random}(\text{size}(D_j)) \oplus Levy(\beta_j)$$

$$\sim (\text{gen} - \text{ite})/\text{gen} * \frac{u_j}{|v_j|^{1/\beta}} \quad (17)$$

where u and v are normal distributed. That is, $u \sim N(0, \sigma_u^2)$, $v \sim N(0, \sigma_v^2)$ with

$$\sigma_u = \left(\frac{\Gamma(1 + \beta) \sin(\pi \cdot \beta/2)}{\Gamma((1 + \beta)/2) \cdot \beta \cdot 2^{(\beta-1)/2}} \right)^{1/\beta}, \quad \sigma_v = 1 \quad (18)$$

where the Γ is the standard Gamma function, $\text{stepsize} * (x_{r1,j}^m - x_{r2,j}^m)$ is added to update the selected best individual to find a new individual. And the simulation studies in the next section will verify its efficiency in searching for a superior solution.

3) TREATMENT MECHANISM OF MULTITUDINOUS AND COMPLEX CONSTRAINTS

The equality constraints and the inequality constrains of dependent variables in IENGs-M system are all non-linear functions of the control variables. Therefore, the multi-objective problem is a multitudinous and complex constraints optimization problem. How to deal with the equality and inequality constraints is an important difficulty to be solved. In this paper, a mixed constraints handling mechanism is proposed. The handling mechanism adopts the repair strategy and penalty terms to tackle the constraints. The repair strategy deals with the upper and lower bounder constraints of

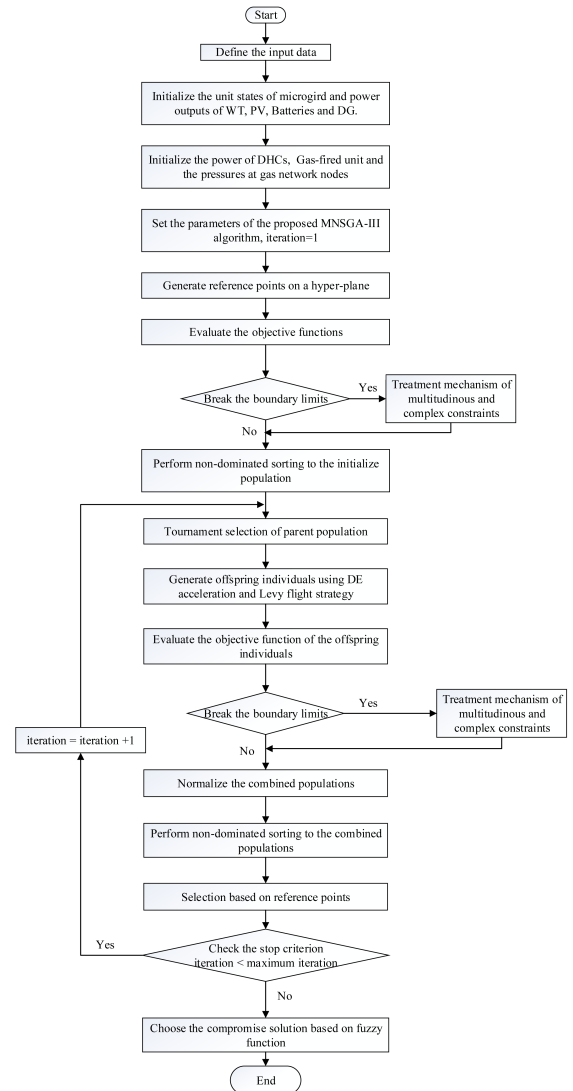


FIGURE 3. The flowchart of the MSGA-III algorithm for the day-ahead scheduling problem of IENGs-M.

control variables. Within the repair strategy, the value of control variables can be satisfied through the resetting operation shown as formula (19) during the solution procedures. The repair strategy to the equality of electricity power flow at each bus is carried out through load flow calculation. The rest constraints of inequality contain transmission lines loading, gas well capacities, compression ratio. These constraints are added to the objective function in form of the quadratic penalty terms. Therefore, the objective function can be augmented as follows (20):

$$x = \begin{cases} x^{\min} & \text{if } x < x^{\min} \\ x & \text{if } x^{\min} \leq x \leq x^{\max} \\ x^{\max} & \text{if } x > x^{\max} \end{cases} \quad (19)$$

$$f_k^M = f_k + \eta \sum_{i=1}^{NL} (\text{fun}_{vio}(S_{li}))^2 + \psi \sum_{i=1}^{N_3} (\text{fun}_{vio}(Q_{W,t}))^2 + \chi (\text{fun}_{vio}(R_i))^2 \quad (20)$$

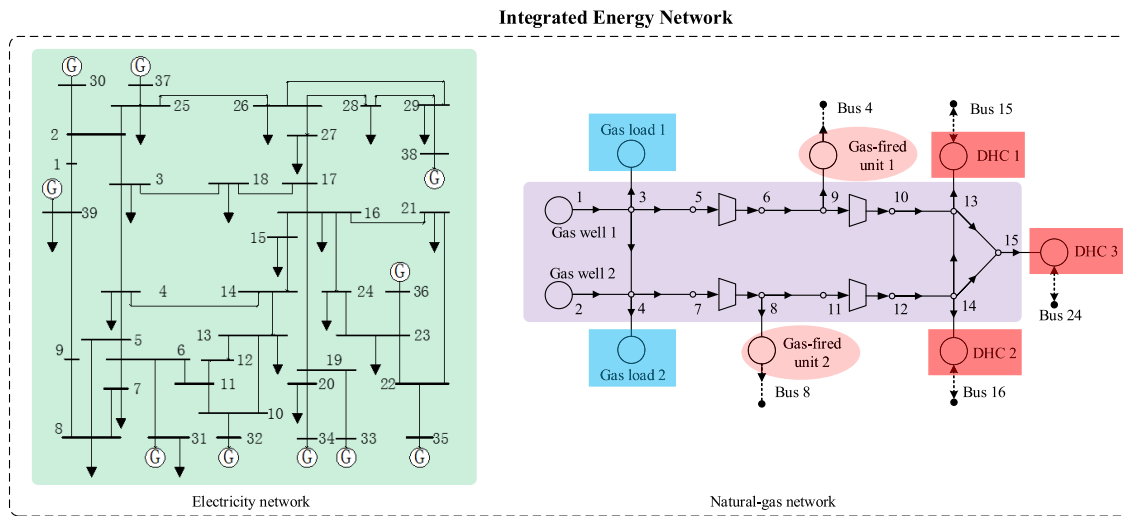


FIGURE 4. The 15-node gas network coupled with 39-bus system including microgrid of large test system.

where η , ψ and χ are the defined as penalty factors. $fun_{vio}(x)$ represents the violation function of the constraints x . In this paper, η , ψ and χ are set 50000.

4) DETAIL STEPS OF MNSGA-III FOR THE DAY-AHEAD SCHEDULING PROBLEM OF IENGs-M

According to the description in the previous section, the flowchart of the proposed method to solve the day-ahead scheduling problem of IENGs-M is expressed in Fig. 3.

IV. DECISION MAKING FOR A FINAL OPTIMAL SOLUTION

In general, the objectives in multi-objective problems usually can't be minimized simultaneously for the reason they conflict with each other. Therefore, one solution can't be said to be better than the other according to their fitness. When the final non-dominated solutions are obtained, it's vital to choose the best compromise solution in the decision making process. In this paper, the fuzzy membership approach is applied to find out the best compromise solution from the non-dominated solutions of the Pareto front. Due to the imprecise nature of the decision make's judgment, the i th objective function f_i of the individual k is defined as follows:

$$\mu_i^k = \begin{cases} 1 & \text{if } f_i < f_i^{\min} \\ \frac{f_i^{\max} - f_i}{f_i^{\max} - f_i^{\min}} & \text{if } f_i^{\min} \leq f_i \leq f_i^{\max} \\ 0 & \text{if } f_i > f_i^{\max} \end{cases} \quad (21)$$

where f_i^{\max} and f_i^{\min} represent the maximum and minimum values of the i th objective function, respectively.

For each non-dominated solution, the sum of the membership function values ($\mu_1^k, \mu_2^k, \dots, \mu_M^k$) is calculated in order to measure the effectiveness of the solution in satisfying the objectives. The normalized value of membership function can

be formulated as:

$$\mu^k = \frac{\sum_{i=1}^M \phi_i \mu_i^k}{\sum_{k=1}^N \sum_{i=1}^M \phi_i \mu_i^k} \quad (22)$$

where M is the number of objectives considered, N is the number of non-dominated solutions, ϕ_i is the weight factor for the i th objective function. In this paper, we consider ϕ_i is 1. The solution with the maximum membership function (μ^k) is selected as the best compromise solution.

V. SIMULATION RESULTS

A. SYSTEM DESCRIPTION

In this section, simulation studies are conducted to verify the performance of the proposed multi-objective optimization algorithm. Simulation studies are carried out on the modified IEEE 39-bus system and 15-node gas system, which is depicted in Fig. 4.

The two network are connected via three DHCs and two gas-fired units. DHCs are located at node 13, 14, 15 of gas network and bus 15, 16, 24 of electricity network. Gas-fired units are located at node 8, 9 of gas network and bus 8, 4 of electricity network. The detail parameter data can be found in [25]–[28]. The scheduling horizon is 24h. The day curves of electricity demand, gas demand, heating demand, cooling demand as well as wind speed and illumination intensity are summarized in Fig. 5 and Fig. 6.

In the electricity network, the power configurations of each microgrid are shown in Table 1. The predicted load demand of each time period is equally distributed to all PQ buses of the system. WT, PV, Battery don't produce atmospheric pollutants during power generation. Therefore, we just need to take the pollution emission of DG and natural gas consumed devices (gas-fired generators and DHCs) into consideration. The pollutant emission factors and the environmental values of different kinds of pollutants are summarized in Table 2.

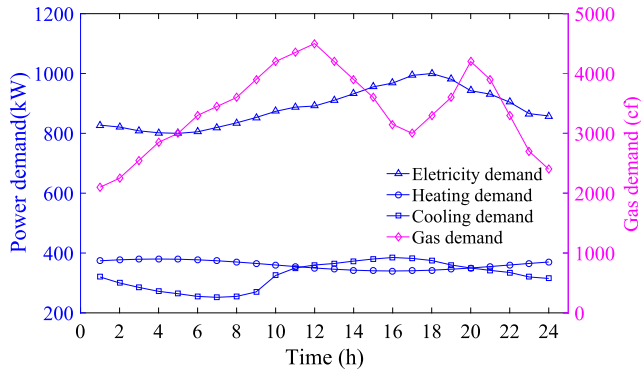


FIGURE 5. The day curves of electricity demand, gas demand, heating and cooling demand.

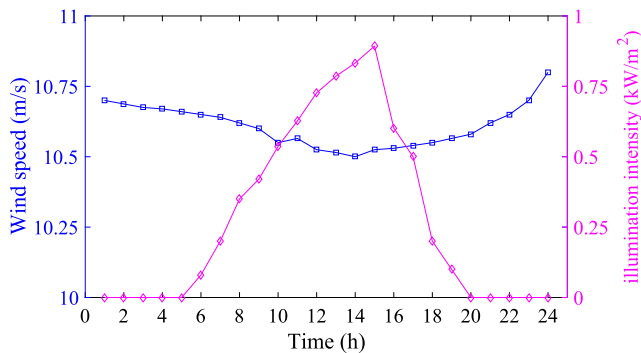


FIGURE 6. The day curves of wind speed and illumination intensity.

TABLE 1. The configurations of each microgrid.

| Type | Wind turbine | Photovoltaic | Battery | Diesel generator |
|--------|--------------|--------------|---------|------------------|
| Number | 3 | 3 | 1 | 1 |

TABLE 2. Pollutant emission factors and cost factors.

| Type | Unit | Pollutant | | | |
|---------------------|-------|-----------|-----------------|-----------------|-----------------|
| | | CO | CO ₂ | NO ₂ | SO ₂ |
| DG | g/kWh | 0.1083 | 623 | 2.88 | 6.48 |
| Natural gas | g/kWh | 0.1702 | 184.0829 | 0.6188 | 0.000928 |
| Environmental value | \$/kg | 0.145 | 0.004125 | 1.25 | 0.875 |

B. ALGORITHMS COMPARISONS

In terms of algorithms, in order to demonstrate the validity and effectiveness of the MNSGA-III, 51 independent runs are carried out with comparison to the other two algorithms (NSGA-II and NSGA-III) for the coordinated operation of IENGSM system, and their parameters are chosen as the same with each other.

Applying the proposed MNSGA-III, the multi-objective optimization problem is optimized with comparisons with the NSGA-II and the NSGA-III. Fig. 7 shows the best Pareto fronts obtained by MNSGA-III and the other two algorithms. As shown in this figure, it is obvious that MNSGA-III outperforms the NSGA-II and the NSGA-III in terms of searching for better converged and more evenly distributed

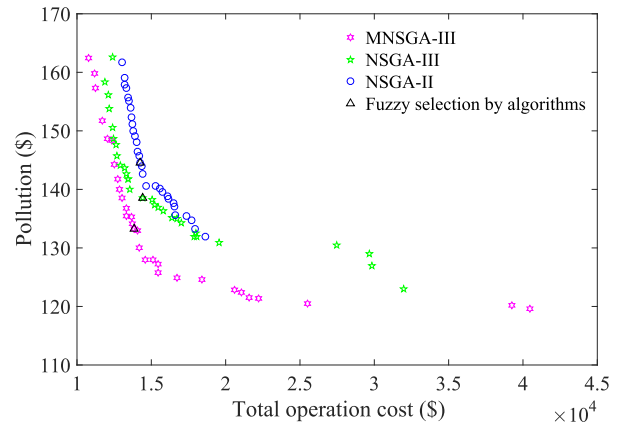


FIGURE 7. The obtained Pareto optimal front by using different algorithms.

non-dominated solutions in case of the coordinated operation of IENGSM considering total operation cost and the pollution.

For the sake of brevity, the fuzzy function is applied to select the best compromise solution in these alternatives. The objective values associated with the best compromise solution acquired by different algorithms are present in Table 3. Judging from Table 3, it can be seen that best value of total operation cost by using MNSGA-III is 1.2844×10^4 \$, with an average cost of 1.3527×10^4 \$ and a worst value of 1.4271×10^4 \$ which are less in comparison to the corresponding results obtained by the other two algorithms. The best value of pollution by using MNSGA-III is 131.918 \$, with an average cost of 135.0643 \$ and a worst value of 139.2679 \$ which are also less in comparison to the corresponding results obtained by the other two algorithms.

In order to more intuitively reflect the improved effect of the Pareto frontier obtained by proposed MNSGA-III, we compared the results of different algorithms with several important indicators which include SP-Metric, HV-Metric, I_D -Metric, and H_D -Metric. These indicators mainly consider the performance of multi-objective optimization algorithms from two aspects: convergence and diversity. Not only that, when we are analyzing these indicators, Wilcoxon signed rank test is executed at a significance level of 0.05 between the proposed MNSGA-III and those by other reported methods. In addition, we use some notations to clarify the comparison results. (1) The p-value of the Wilcoxon signed rank is the probability of a hypothesis of equal median of two-sided test. (2) The h-value is the result of the Wilcoxon signed rank. If $h = 0$, it indicates that the median of the difference between the proposed MNSGA-III and the compared algorithms is zero. Otherwise, there is a significant difference, if $h = 1$.

The results obtained by these metrics comparisons are presented in Table 4. As shown in the table, the proposed MNSGA-III can obtain more Pareto-optimal solutions than the NSGA-II and NSGA-III under the same number of iterations. Moreover, the SP-Metric and HV-Metric show that the solutions obtained by MNSGA-III have better quality of

TABLE 3. The stability analysis for the objective values associated with the best compromise solution using different algorithms.

| Algorithms | Type | Best value | Worst value | Mean value | Variance | Standard deviation |
|------------|---------------|----------------------|----------------------|----------------------|----------|--------------------|
| MNSGA-III | cost(\$) | 1.2844×10^4 | 1.4271×10^4 | 1.3527×10^4 | 1974.7 | 44.4378 |
| | pollution(\$) | 131.918 | 139.2679 | 135.0643 | 4.8751 | 2.2080 |
| NSGA-III | cost(\$) | 1.3688×10^4 | 1.6138×10^4 | 1.4825×10^4 | 8238.6 | 90.7667 |
| | pollution(\$) | 138.5294 | 152.6200 | 142.2907 | 12.7524 | 3.5711 |
| NSGA-II | cost(\$) | 1.3625×10^4 | 1.5248×10^4 | 1.4517×10^4 | 6201.3 | 78.7483 |
| | pollution(\$) | 139.0834 | 147.4453 | 143.9809 | 4.3340 | 2.0818 |

TABLE 4. The stability analysis for the objective values associated with the best compromise solution using different algorithms in Case I.

| Metrics | MNSGA-III | | NSGA-III | | p | | NSGA-II | | p | |
|---------------|---------------|--------|----------|--------|-----------|---|---------|--------|-----------|---|
| | Mean | Std | Mean | Std | | h | Mean | Std | | h |
| SP-Metric | 0.8358 | 0.0651 | 0.8658 | 0.0454 | 0.1206 | 0 | 0.8996 | 0.0522 | 0.0298 | 1 |
| HV-Metric | 0.8569 | 0.0360 | 0.6549 | 0.0458 | 4.3778E-4 | 1 | 0.6458 | 0.0488 | 4.3778E-4 | 1 |
| I_D -Metric | 0.0035 | 0.0016 | 0.0267 | 0.0065 | 4.3391E-4 | 1 | 0.0256 | 0.0082 | 4.3391E-4 | 1 |
| H_D -Metric | 0.0847 | 0.0507 | 0.5710 | 0.2228 | 4.3391E-4 | 1 | 0.5980 | 0.2095 | 4.3391E-4 | 1 |

Bold values correspond to the best values

convergence and diversity than those obtained by the two algorithms. Meanwhile, the smaller the I_D -Metric and H_D -Metric of MNSGA-III is, the better the distribution of the solutions acquired by MNSGA-III is. Not only that, the median differences between MNSGA-III and the other two compared algorithms are significant in the test case shown in the Table 4. As a consequence, it can be concluded that the improvement of the MNSGA-III can guarantee that it can find a better set of Pareto-optimal solutions compared to the NSGA-II and NSGA-III.

VI. CONCLUSION

This paper has proposed an effective MNSGA-III multi-objective algorithm to solve the complicated constrained optimization problem. In order to validate the applicability and performance of the MNSGA-III algorithm in real-world problems, the MNSGA-III is tested on the day-ahead scheduling problem of IENGs-M system.

Compared with the NSGA-II and NSGA-III, the performance of MNSGA-III on the indicator of SP-Metric, HV-Metric, I_D -Metric, H_D -Metric and the number of Pareto-optimal solutions is better, which means that the MNSGA-III is more efficient in searching for the superior Pareto-optimal solutions in terms of convergence and diversity.

Furthermore, a decision making method based on fuzzy function approach has been applied to determine the best compromise solution for the IENGs-M. From the best compromise solutions of MNSGA-III and the other reported algorithms in this paper, it also can be concluded that the proposed algorithm is more efficient in solving the optimal operation problem of the IENGs-M.

REFERENCES

[1] J. Li, S. Wang, L. Ye, and J. Fang, "A coordinated dispatch method with pumped-storage and battery-storage for compensating the variation of wind power," *Protection Control Mod. Power Syst.*, vol. 3, no. 1, pp. 21–34, Dec. 2018.

[2] H. Wang, Z. Lei, X. Zhang, B. Zhou, and J. Peng, "A review of deep learning for renewable energy forecasting," *Energy Convers. Manage.*, vol. 198, Oct. 2019, Art. no. 111799.

[3] D. Xu, Q. Wu, B. Zhou, C. Li, L. Bai, and S. Huang, "Distributed multi-energy operation of coupled electricity, heating and natural gas networks," *IEEE Trans. Sustain. Energy*, early access, Dec. 20, 2019, doi: 10.1109/TSTE.2019.2961432.

[4] H.-Z. Wang, G.-Q. Li, G.-B. Wang, J.-C. Peng, H. Jiang, and Y.-T. Liu, "Deep learning based ensemble approach for probabilistic wind power forecasting," *Appl. Energy*, vol. 188, pp. 56–70, Feb. 2017.

[5] A. Quelhas, E. Gil, J. D. McCalley, and S. M. Ryan, "A multiperiod generalized network flow model of the US integrated energy system: Part I—Model description," *IEEE Trans. Power Syst.*, vol. 22, no. 2, pp. 829–836, May 2007.

[6] M. Chaudry, N. Jenkins, and G. Strbac, "Multi-time period combined gas and electricity network optimisation," *Electr. Power Syst. Res.*, vol. 78, no. 7, pp. 1265–1279, Jul. 2008.

[7] M. Qadrdan, M. Chaudry, J. Wu, N. Jenkins, and J. Ekanayake, "Impact of a large penetration of wind generation on the GB gas network," *Energy Policy*, vol. 38, no. 10, pp. 5684–5695, Oct. 2010.

[8] A. Alabdulwahab, A. Abusorrah, X. Zhang, and M. Shahidehpour, "Coordination of interdependent natural gas and electricity infrastructures for firming the variability of wind energy in stochastic day-ahead scheduling," *IEEE Trans. Sustain. Energy*, vol. 6, no. 2, pp. 606–615, Apr. 2015.

[9] P. N. Biskas, N. G. Kanelakis, A. Papamathaiou, and I. Alexandridis, "Coupled optimization of electricity and natural gas systems using augmented Lagrangian and an alternating minimization method," *Int. J. Electr. Power Energy Syst.*, vol. 80, pp. 202–218, Sep. 2016.

[10] H. Wang, J. Ruan, Z. Ma, B. Zhou, X. Fu, and G. Cao, "Deep learning aided interval state prediction for improving cyber security in energy Internet," *Energy*, vol. 174, pp. 1292–1304, May 2019.

[11] S. He, Q. H. Wu, and J. R. Saunders, "Group search optimizer: An optimization algorithm inspired by animal searching behavior," *IEEE Trans. Evol. Comput.*, vol. 13, no. 5, pp. 973–990, Oct. 2009.

[12] M. A. Hassan and M. A. Abido, "Optimal design of microgrids in autonomous and grid-connected modes using particle swarm optimization," *IEEE Trans. Power Electron.*, vol. 26, no. 3, pp. 755–769, Mar. 2011.

[13] S. Wang, X. Fan, L. Han, and L. Ge, "Improved interval optimization method based on differential evolution for microgrid economic dispatch," *Electr. Power Compon. Syst.*, vol. 43, no. 16, pp. 1882–1890, Oct. 2015.

[14] B. Shaw, V. Mukherjee, and S. P. Ghoshal, "A novel opposition-based gravitational search algorithm for combined economic and emission dispatch problems of power systems," *Int. J. Electr. Power Energy Syst.*, vol. 35, no. 1, pp. 21–33, Feb. 2012.

[15] H. Wang, Z. Lei, X. Zhang, J. Peng, and H. Jiang, "Multiobjective reinforcement learning-based intelligent approach for optimization of activation rules in automatic generation control," *IEEE Access*, vol. 7, pp. 17480–17492, 2019.

- [16] K. Deb and H. Jain, "An evolutionary many-objective optimization algorithm using reference-point-based nondominated sorting approach, part I: Solving problems with box constraints," *IEEE Trans. Evol. Comput.*, vol. 18, no. 4, pp. 577–601, Aug. 2014.
- [17] H. Jain and K. Deb, "An evolutionary many-objective optimization algorithm using reference-point based nondominated sorting approach, part II: Handling constraints and extending to an adaptive approach," *IEEE Trans. Evol. Comput.*, vol. 18, no. 4, pp. 602–622, Aug. 2014.
- [18] M. W. Mkaouer, M. Kessentini, M. ÓCinnéide, S. Bechikh, and K. Deb, "High dimensional search-based software engineering: Finding trade-offs among 15 objectives for automating software refactoring using NSGA-III," in *Proc. Conf. Genetic Evol. Comput. (GECCO)*, 2014, pp. 1263–1270.
- [19] C. Essayeh, M. R. E. Fenni, and H. Dahmouni, "Optimization of energy exchange in microgrid networks: A coalition formation approach," *Protection Control Mod. Power Syst.*, vol. 4, no. 1, pp. 296–305, Dec. 2019.
- [20] X. Yuan, H. Tian, Y. Yuan, Y. Huang, and R. M. Ikram, "An extended NSGA-III for solution multi-objective hydro-thermal-wind scheduling considering wind power cost," *Energy Convers. Manage.*, vol. 96, pp. 568–578, May 2015.
- [21] B. Ji, X. Yuan, and Y. Yuan, "Orthogonal design-based NSGA-III for the optimal lockage co-scheduling problem," *IEEE Trans. Intell. Transp. Syst.*, vol. 18, no. 8, pp. 2085–2095, Aug. 2017.
- [22] C. Chen, Y. Yuan, and X. Yuan, "An improved NSGA-III algorithm for reservoir flood control operation," *Water Resource Manage.*, vol. 31, no. 14, pp. 4469–4483, Nov. 2017.
- [23] X. Bi and C. Wang, "An improved NSGA-III algorithm based on objective space decomposition for many-objective optimization," *Soft Comput.*, vol. 21, no. 15, pp. 4269–4296, Aug. 2017.
- [24] R. H. Bhesdadiya, I. N. Trivedi, P. Jangir, N. Jangir, and A. Kumar, "An NSGA-III algorithm for solving multi-objective economic/environmental dispatch problem," *Cogent Eng.*, vol. 3, no. 1, 2016, Art. no. 1269383.
- [25] J. H. Zheng, Q. H. Wu, and Z. X. Jing, "Coordinated scheduling strategy to optimize conflicting benefits for daily operation of integrated electricity and gas networks," *Appl. Energy*, vol. 192, pp. 370–381, Apr. 2017.
- [26] S. An, Q. Li, and T. W. Gedra, "Natural gas and electricity optimal power flow," in *Proc. IEEE PES Transmiss. Distrib. Conf. Expo.*, Sep. 2004, pp. 138–143.
- [27] A. Martinez-Mares and C. R. Fuente-Esquivel, "A unified gas and power flow analysis in natural gas and electricity coupled networks," *IEEE Trans. Power Syst.*, vol. 27, no. 4, pp. 2156–2166, Nov. 2012.
- [28] L. L. Wu, Q. H. Wu, Z. X. Jing, F. Wei, S. Deng, and X. X. Zhou, "Optimal power and gas dispatch of the integrated electricity and natural gas networks," in *Proc. IEEE Innov. Smart Grid Technol. Asia (ISGT-Asia)*, Nov. 2016, pp. 244–249.



C. Q. WU received the B.E. degree in electrical engineering and its automation from Guangxi University, Nanning, China, in 2019. She is currently pursuing the master's degree in electrical engineering and its automation from the South China University of Technology, Guangzhou, China. Her research interests include the area of optimization algorithms, and decision making methods and their applications on integrated energy systems.



J. HUANG received the B.E. and master's degrees in electrical engineering and its automation from the South China University of Technology (SCUT), Guangzhou, China in 2016 and 2019, respectively. His research interests include the area of optimization algorithms and their applications on integrated energy systems.



Y. LIU (Member, IEEE) received the B.E. and Ph.D. degrees in electrical engineering from the South China University of Technology (SCUT), Guangzhou, China, in 2012 and 2017, respectively. He is currently a Lecturer with the School of Electric Power Engineering, SCUT. His research interests include the areas of power system stability analysis and control, control of wind power generation systems, and nonlinear control theory. He has authored or coauthored more than 30 peer-reviewed SCI journal articles.



Q. H. WU (Fellow, IEEE) received the M.Sc. (Eng.) degree in electrical engineering from the Huazhong University of Science and Technology, Wuhan, China, in 1981, and the Ph.D. degree in electrical engineering from The Queen's University of Belfast (QUB), Belfast, U.K., in 1987. From 1981 to 1984, he was a Lecturer in electrical engineering with the Huazhong University of Science and Technology. He was a Research Fellow and subsequently a Senior Research Fellow with QUB, from 1987 to 1991. He joined the Department of Mathematical Sciences, Loughborough University, Loughborough, U.K., in 1991, as a Lecturer, subsequently he was appointed as a Senior Lecturer. In September 1995, he joined The University of Liverpool, Liverpool, U.K., to take up his appointment to the Chair of electrical engineering in the Department of Electrical Engineering and Electronics. He is currently with the School of Electric Power Engineering, South China University of Technology, Guangzhou, China, as a Distinguished Professor and the Director of the Energy Research Institute. He has authored or coauthored more than 440 technical publications, including 220 journal articles, 20 book chapters, and 3 research monographs published by Springer. He is a Fellow of IET, Chartered Engineer, and a Fellow of InstMC. His research interests include nonlinear adaptive control, mathematical morphology, evolutionary computation, power quality, and power system control and operation.



J. H. ZHENG (Member, IEEE) received the B.E. degree in electrical engineering from the Huazhong University of Science and Technology, Wuhan, China, in 2012, and the Ph.D. degree in electrical engineering from the South China University of Technology (SCUT), Guangzhou, China, in 2017. He is currently a Lecturer with SCUT. He has authored or coauthored more than 40 peer-reviewed SCI journal articles. His research interests include the area of optimization algorithms, and decision making methods and their applications on integrated energy systems.

...